SAMS, 1993, Vol. 12, pp. 101–123
Reprints available directly from the publisher
Photocopying permitted by licence only

STATISTICAL MODELLING OF ROBOTIC MANIPULATORS

J. A. TENREIRO MACHADO and ALEXANDRA M. S. F. GALHANO

Faculty of Engineering of the University of Porto, Department of Electrical and Computer Engineering, Portugal

(Received December 19, 1992)

The article presents a new approach to the analysis and design of robotic manipulators. The novel feature resides on a non-standard formulation to the modelling problem. Usually, system descriptions are based on a set of differential equations which, due to their nature, lead to very precise results and strategies but require laborious computations. This motivates the need of alternative models based on other mathematical concepts. The proposed statistical method gives clear guidelines towards the robot kinematic and dynamic optimsation. Furthermore, the results point out structural characteristics of the trajectory planning algorithm as well as ideal-actuator properties.

KEY WORDS Robotics, manipulators, modelling, statistics.

1. INTRODUCTION

Mechanical manipulators are developed according to engineering and scientific principles that are based on fundamental concepts such as those arising from mathematics and physics. Based on these formulations, the first step on the study of a given physical phenomena is the development of an adequate model. Manipulators are a system where we have for fundamental concepts the differential and matrix calculus and the classical Newtonian physics, while the model corresponds to the standard kinematic and dynamic descriptions. Nevertheless, other classes of phenomena such as quantum physics and thermodynamics are studied using different concepts. Quantum physics requires the use of statistical methods while thermodynamics can be studied both through classical and statistical methods. These facts suggest that, for a given problem, we may develop different models each with its own merits and drawbacks. This paper presents a framework where these problems are addressed for robotic manipulators. We develop a new modelling approach based on a statistical formalism. These concepts are then illustrated on a simple mechanical joint-actuated arm. This example reveals not only the capabilities of the new method but also the limitations of usual robot structures. In order to develop the method we organise this paper as follows. Section two formulates the new fundamental modelling concepts. Section three illustrates the application of the statistical method to the kinematics and dynamics of mechanical manipulators. Finally, section four presents the main conclusions.

2. ON THE STATISTICAL MODELLING OF MECHANICAL MANIPULATORS

The classical modelling of mechanical manipulators is well known. For an n degrees of freedom (d.o.f.) robot the kinematics is described by a set of non-linear equations that describes the transformation $(\mathbf{p}, \dot{\mathbf{p}}, \ddot{\mathbf{p}}) \rightarrow (\mathbf{q}, \dot{\mathbf{q}}, \ddot{\mathbf{q}})$:

$$\mathbf{q} = \psi(\mathbf{p}) \tag{1a}$$

$$\dot{\mathbf{q}} = \left[\frac{\partial \psi(\mathbf{q})}{\partial \mathbf{p}}\right] \dot{\mathbf{p}} \tag{1b}$$

$$\ddot{\mathbf{q}} = \left[\frac{\partial \psi(\mathbf{q})}{\partial \mathbf{p}}\right] \ddot{\mathbf{p}} + \left[\frac{\partial^2 \psi(\mathbf{q})}{\partial \mathbf{p}^2}\right] \dot{\mathbf{p}}^2 \tag{1c}$$

where:

$$\mathbf{p} = [p_1, \cdots, p_n]^T, \quad \dot{\mathbf{p}} = [\dot{p}_1, \cdots, \dot{p}_n]^T, \quad \ddot{\mathbf{p}} = [\ddot{p}_1, \cdots, \ddot{p}_n]^T \tag{2a}$$

$$\mathbf{q} = [q_1, \cdots, q_n]^T, \quad \dot{\mathbf{q}} = [\dot{q}_1, \cdots, \dot{q}_n]^T, \quad \ddot{\mathbf{q}} = [\ddot{q}_1, \cdots, \ddot{q}_n]^T \tag{2b}$$

are the positions, velocities and accelerations in the operational and joint spaces, respectively.

The second level of system modelling consists on the dynamics that describes the transformation $(\mathbf{q}, \dot{\mathbf{q}}, \ddot{\mathbf{q}}) \rightarrow \mathbf{T}$:

$$\mathbf{T} = \mathbf{T}_G + \mathbf{T}_C + \mathbf{T}_I \tag{3a}$$

$$\mathbf{T}_G = \mathbf{G}(\mathbf{q}) \tag{3b}$$

$$\mathbf{T}_C = \mathbf{C}(\mathbf{q}, \dot{\mathbf{q}}) \tag{3c}$$

$$\mathbf{T}_I = \mathbf{I}(\mathbf{q})\ddot{\mathbf{q}} \tag{3d}$$

where $\mathbf{T}, \mathbf{T}_G, \mathbf{T}_C$ and $\mathbf{T}_I$ are the n-dimensional vectors of the total, gravitational, Coriolis/centripetal and inertial torques at the joints, respectively. However, a more sound consideration of the whole theme reveals that such equations are far from achieving a comprehensive formulation. In fact, the classical methodology leads to difficulties on the various steps of system modelling. The model equations, namely for the dynamics, are very complex for a six d.o.f. manipulator [1-3]. This makes impossible the manual deduction of the model of a typical industrial robot and leads to the requirement of an automatic, computer-based, derivation of the corresponding mathematical expressions [4-8]. A second problem resides on the high computational burden posed by the resulting system equations. Figure 1 shows a common example of this state of affairs. The real-time computation of the highly simplified equations of the dynamics of the PUMA 560 [9-10] requires 11 sines/cosines 89 additions and 151 multiplications for each point which still corresponds to a heavy burden for present day computer systems. A third difficulty is found when applying the classical model on the optimisation of the manipulator structure [11-16] and the development of efficient trajectory planning algorithms [17-18]. The optimising procedures are complex and the results are not clear.

These observations motivate the re-evaluation of the concepts in use. Expressions (1) and (3) involve a plethora of variables and parameters that give rise to a

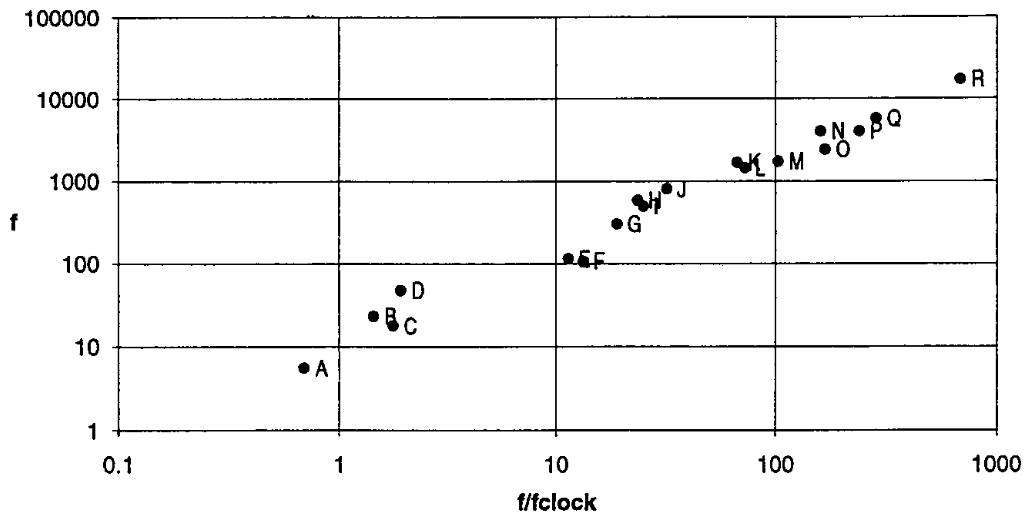

Figure 1 Calculation frequency f versus the index f/f_{clock} ('normalized frequency') of the Puma 560 simplified dynamics for several computing systems using floating point operations with eight bytes precision.

	System	*Processor/Coprocessor*	f_{clock}	*O.S.*	*Language*
A	IBM PS/2	8086	8 MHz	MSDOS 3.3	TC V2.0
B	IBM PS/2	80386 SX	16 MHz	MSDOS 3.3	TC V2.0
C	IBM PS/2	80286	10 MHz	MSDOS 3.3	TC V2.0
D	IBM PS/2	80386	25 MHz	MSDOS 3.3	TC V2.0
E	IBM PS/2	80286/80287	10 MHz	MSDOS 3.3	TC V2.0
F	IBM PS/2	8086/8087	8 MHz	MSDOS 3.3	TC V2.0
G	IBM PS/2	80386 SX/80387 SX	16 MHz	MSDOS 3.3	TC V2.0
H	IBM PS/2	80386/80387	25 MHz	MSDOS 3.3	TC V2.0
I	SUN 3/60	68020/68881	20 MHz	UNIX 4.2	GNU C V1.25
J	Apollo DN 3500	68030/68882	25 MHz	BSD 4.2 DO/IX	System C
K	IBM PS/2	80486	25 MHz	MSDOS 3.3	TC V2.0
L	T800-20	IMS T800-20	20 MHz		Occam 2
M	AViiON AVX 300	88100	16.7 MHz	DG/UX 4.2	System C
N	NEXT CUBE	68040	25 MHz	Nextstep 2.1 Mach 2.5	GNU C V1.36
O	SUN 4/110	SPARC	14.3 MHz	UNIX 4.3.2	System C
P	DECSTATION 3100	MIPS 2000/2010	16.7 MHz	Ultrix 3.1	System C
Q	SUN 4/60 SPARCSt.1	SPARC	20 MHz	SUN 4.0.3	System C
R	IBM 6000 St.530	IBM Power System/6000	25 MHz	AIX V3.1	System C

gigantic number of possible combinations of values. Therefore, in order to overcome implementation problems, alternative concepts are required. Statistics is a mathematical tool well adapted to this type of problem. If with this method, we lose the 'certainty' of the deterministic model, we gain a simpler and more intuitive viewpoint. This approach has already been used by other researchers [19–20] in some restricted classes of problems. In the sequel we refer to the new approach, as the statistical model [21–23] to stress the contrast with the standard method. Our modelling procedure comprises:

- The statistical description of a set of input variables (i.v.'s), that is variables that are free to change independently.
- The statistical description of a set of output variables (o.v.'s), that is, variables that are functions of the previous ones.

- A set of parameters that are to be optimised in the design stage.

The above definition allows a considerable freedom in the choice of each set. In the present case, the distribution of the relevant variables through the three referred sets is established as follows:

- The i.v.'s of the kinematic system are $\{\mathbf{p}, \dot{\mathbf{p}}, \ddot{\mathbf{p}}\}$. This option enables the definition of the required kinematic performances on the operational space that are more natural to the designer.
- The o.v.'s of the kinematic system are $\{\mathbf{q}, \dot{\mathbf{q}}, \ddot{\mathbf{q}}\}$ which play, also, the role of i.v.'s of the dynamic model. In this way we establish a relationship between kinematics and dynamics.
- The o.v.'s of the dynamics consists on the required joint torques $\{\mathbf{T}\}$.
- The set of parameters consists of link lengths, masses and inertias.

In other words, we are stating that in the kinematics (dynamics), $\mathbf{p}, \dot{\mathbf{p}}$ and $\ddot{\mathbf{p}}$ ($\mathbf{q}, \dot{\mathbf{q}}$ and $\ddot{\mathbf{q}}$) are considered as independent random variables that have probability density functions (p.d.f's) similar to the histograms of a long run sampling, while $\mathbf{q}, \dot{\mathbf{q}}$ and $\ddot{\mathbf{q}}$ ($\mathbf{T}$) are the corresponding random dependent variables. The statistical description of the variables does not consider the (implicit) time variable. In this way, variables that are related through the time derivative operator—positions, velocities and accelerations—are considered independent of each other. This means that the statistical formulation does not answer questions such as system stability or its bandwidth but, on the other hand, may provide a useful tool for the study of time-independent properties.

3. A STATISTICAL MODEL FOR THE 2R MANIPULATOR

In this section we adopt the 2R joint-actuated manipulator (Figure 2) as the support for the development and implementation of the new modelling concepts. In the first sub-section we begin by introducing our approach in the kinematics. Then, in the second sub-section we analyse the dynamics and, finally, in the third sub-section we investigate the properties of the global system (i.e. both kinematics and dynamics).

3.1. *The Kinematics*

As mentioned previously, the kinematics consists on the transformation $(\mathbf{p}, \dot{\mathbf{p}}, \ddot{\mathbf{p}}) \to (\mathbf{q}, \dot{\mathbf{q}}, \ddot{\mathbf{q}})$. We begin our study with a experimental numerical-based approach and, in a second stage, we adopt a complementary analytical perspective.

In order to have a statistical description we have to characterise the random variables through appropriate p.d.f's. At this point there is no *a priori* knowledge about the statistical properties of the system. Therefore, we start our experiments with some preliminary assumptions and, in the sequel, we demonstrate the conditions that optimise the kinematic performances.

For $\mathbf{p} = [p_1, p_2]^T$ we consider a bidimensional uniform p.d.f:

$$f_P(\mathbf{p}) = \begin{cases} 0 & p_1^2 + p_2^2 < (l_1 - l_2)^2 \vee (l_1 + l_2)^2 < p_1^2 + p_2^2 \\ (4\pi l_1 l_2)^{-1} & (l_1 - l_2)^2 \leqslant p_1^2 + p_2^2 \leqslant (l_1 + l_2)^2 \end{cases} \tag{4}$$

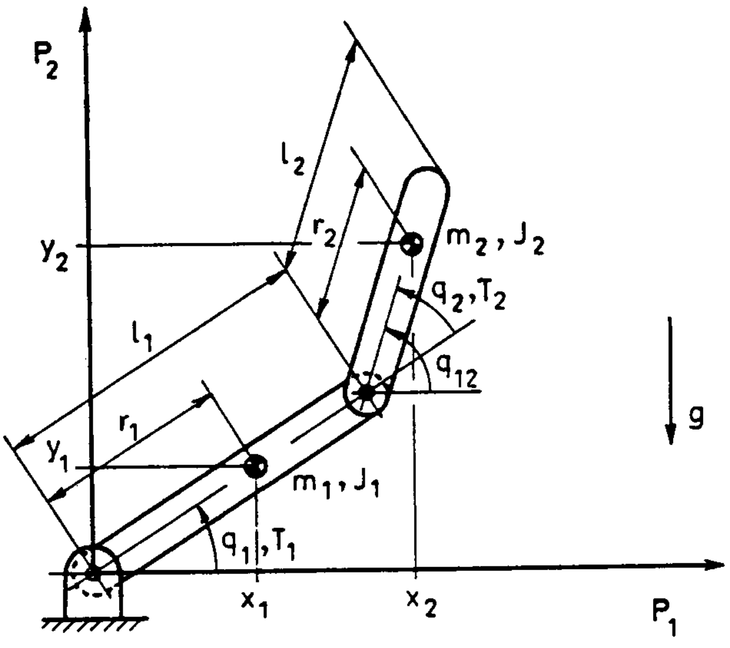

Figure 2 The 2R joint-actuated robot manipulator.

For $\dot{\mathbf{p}} = [\dot{p}_1, \dot{p}_2]^T$ and $\ddot{\mathbf{p}} = [\ddot{p}_1, \ddot{p}_2]^T$ we use bidimensional Gaussian p.d.f.'s with zero mean:

$$f_{\dot{P}}(\dot{\mathbf{p}}) = \frac{1}{2\pi\sigma_{\dot{P}}^2} \exp\left(-\frac{\dot{p}_1^2 + \dot{p}_2^2}{2\sigma_{\dot{P}}^2}\right) \tag{5}$$

$$f_{\ddot{P}}(\ddot{\mathbf{p}}) = \frac{1}{2\pi\sigma_{\ddot{P}}^2} \exp\left(-\frac{\ddot{p}_1^2 + \ddot{p}_2^2}{2\sigma_{\ddot{P}}^2}\right) \tag{6}$$

where $\sigma_{\dot{P}}$ and $\sigma_{\ddot{P}}$ are the standard deviation of $\dot{\mathbf{p}}$ and $\ddot{\mathbf{p}}$, respectively. Moreover, p.d.f's (4)–(6) impose that:

- The random variables $\mathbf{p}$, $\dot{\mathbf{p}}$ and $\ddot{\mathbf{p}}$ are independent of each other.
- $\dot{\mathbf{p}}$ and $\ddot{\mathbf{p}}$ consist on two independent components.

The kinematic o.v.'s have p.d.f's that are related to the previous ones by the expressions:

$$g_Q(\mathbf{q}) = |\mathfrak{J}_P| f_P[\mathbf{q}(\mathbf{p})] \tag{7a}$$

$$g_{Q\dot{Q}}(\mathbf{q}, \dot{\mathbf{q}}) = |\mathfrak{J}_{P\dot{P}}| f_{P\dot{P}}[\mathbf{q}(\mathbf{p}), \dot{\mathbf{q}}(\dot{\mathbf{p}})] \tag{7b}$$

$$g_{Q\dot{Q}\ddot{Q}}(\mathbf{q}, \dot{\mathbf{q}}, \ddot{\mathbf{q}}) = |\mathfrak{J}_{P\dot{P}\ddot{P}}| f_{P\dot{P}\ddot{P}}[\mathbf{q}(\mathbf{p}), \dot{\mathbf{q}}(\dot{\mathbf{p}}), \ddot{\mathbf{q}}(\ddot{\mathbf{p}})] \tag{7c}$$

where the jacobians $\mathfrak{J}_P, \mathfrak{J}_{P\dot{P}}$ and $\mathfrak{J}_{P\dot{P}\ddot{P}}$ are

$$\mathfrak{J}_P = \frac{\partial(\mathbf{p})}{\partial(\mathbf{q})} \tag{8a}$$

$$\mathfrak{J}_{P\dot{P}} = \frac{\partial(\mathbf{p}, \dot{\mathbf{p}})}{\partial(\mathbf{q}, \dot{\mathbf{q}})} \tag{8b}$$

$$\mathfrak{J}_{\mathbf{P}\dot{\mathbf{P}}\ddot{\mathbf{P}}} = \frac{\partial(\mathbf{p}, \dot{\mathbf{p}}, \ddot{\mathbf{p}})}{\partial(\mathbf{q}, \dot{\mathbf{q}}, \ddot{\mathbf{q}})} \tag{8c}$$

Each of the expressions (7) is made of two factors:

- A 'weighting factor'—$\mathfrak{J}_{\mathbf{P}}$, $\mathfrak{J}_{\mathbf{P}\dot{\mathbf{P}}}$ or $\mathfrak{J}_{\mathbf{P}\dot{\mathbf{P}}\ddot{\mathbf{P}}}$—which depend solely on the system kinematic properties.
- An 'excitation' p.d.f—$f_{\mathbf{P}}[\mathbf{q}(\mathbf{p})]$, $f_{\mathbf{P}\dot{\mathbf{P}}}[\mathbf{q}(\mathbf{p}), \dot{\mathbf{q}}(\dot{\mathbf{p}})]$ or $f_{\mathbf{P}\dot{\mathbf{P}}\ddot{\mathbf{P}}}$ $[\mathbf{q}(\mathbf{p}), \dot{\mathbf{q}}(\dot{\mathbf{p}}), \ddot{\mathbf{q}}(\ddot{\mathbf{p}})]$ —which is a measure of the task requirements.

These factors can be interpreted in a system theoretic framework. The jacobians characterise the system intrinsic properties, while the excitation p.d.f's correspond to the system response to the i.v.'s.

In order to test these ideas we decided to perform several numerical experiments with the total manipulator length constant, ($L = l_1 + l_2 = 0.6$), seven robot kinematic configurations (Table I) and nine categories of requirements of $\dot{\mathbf{p}}$ and $\ddot{\mathbf{p}}$ (Table II).

Table I Robot kinematic configurations.

Configuration	*1*	*2*	*3*	*4*	*5*	*6*	*7*
$\mu = l_1/l_2$	0.4	0.6	0.8	1	1.2	1.4	1.6

Table II Requirements of $\dot{\mathbf{p}}$ and $\ddot{\mathbf{p}}$.

Category	*1*	*2*	*3*	*4*	*5*	*6*	*7*	*8*	*9*
$\sigma_{\dot{\mathbf{p}}}$	0.1	0.1	0.1	1	1	1	10	10	10
$\sigma_{\ddot{\mathbf{p}}}$	0.1	1	10	0.1	1	10	0.1	1	10

The 'excitation' of the kinematics with a numerical random sample of i.v.'s obeying p.d.f's (4)–(6) leads to a dependent (six-dimensional sample of $\mathbf{q}$, $\dot{\mathbf{q}}$ and $\ddot{\mathbf{q}}$. Nevertheless, robot joint actuators are independent of each other; therefore, only marginal (one-dimensional) histograms of amplitudes of the o.v.'s have to be analysed which simplifies the subsequent treatment. Figure 3 shows a synoptic diagram of this experimental procedure. From this chart we can conclude, directly, that q_1 and q_2 are statistically independent that is $g_{\mathbf{Q}}(\mathbf{q}) = g_{Q_1}(q_1)g_{Q_2}(q_2)$. In what concerns $\dot{\mathbf{q}}$ and $\ddot{\mathbf{q}}$, to condense its histograms by a scalar index we adopted the difference between the 97.5% and 2.5% percentiles that is, we adopted the 95%-inter-percentile range (IP_{95}). Experiments demonstrated that other values of the inter-percentile lead to similar conclusions. Moreover, the outcoming p.d.f's showed symmetry around zero. Therefore, the results are condensed through IP_{95} but, due to the symmetry, only the positive half is depicted in Figure 4. From the charts of Figures 3 and 4 we conclude that:

- $\dot{q}_1$ and $\dot{q}_2$ have similar results in each group of categories {1, 2, 3}, {4, 5, 6} and {7, 8, 9}. This indicates that, as expected, joint velocities are independent of $\ddot{\mathbf{p}}$.
- $\ddot{q}_1$ and $\ddot{q}_2$ depend both on $\dot{\mathbf{p}}$ and $\ddot{\mathbf{p}}$. Nevertheless, the influence of $\dot{\mathbf{p}}$ is much stronger than the influence of $\ddot{\mathbf{p}}$, particularly for categories 4 to 9. This means

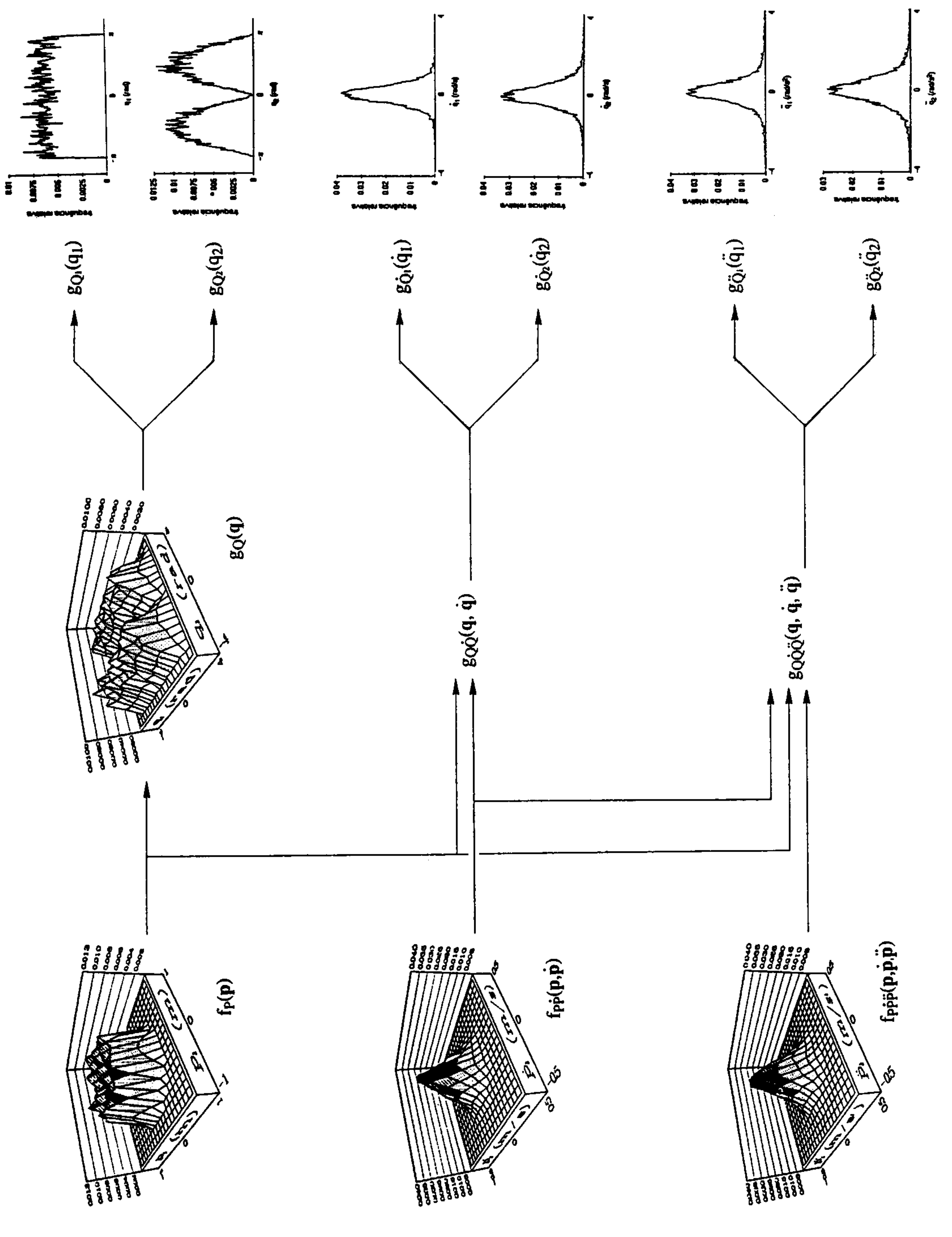

Figure 3 Synoptic diagram of the statistical modelling of the kinematics.

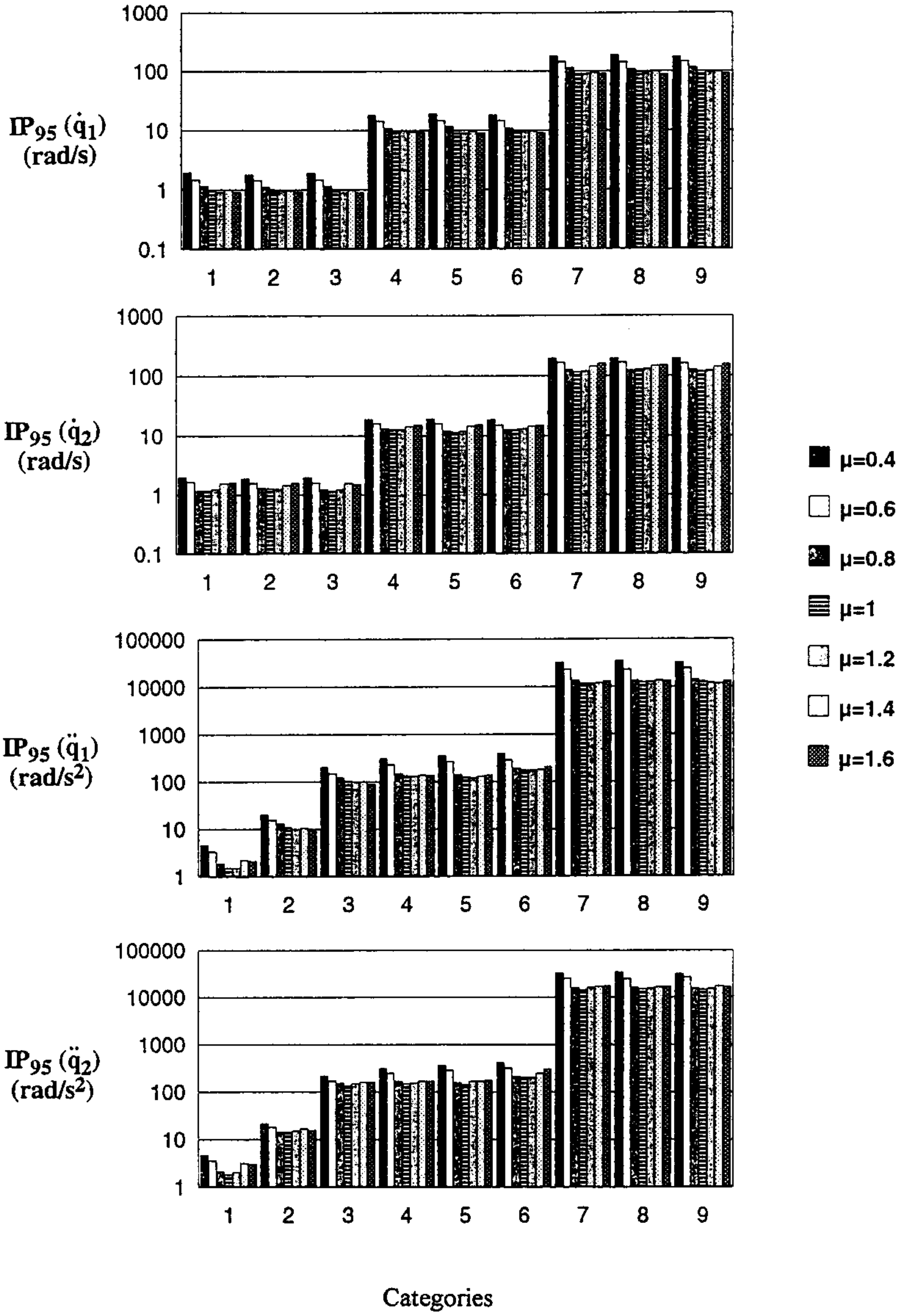

Figure 4 Comparison of the kinematic performances of the 2R manipulator with seven different structures for the p.d.f.'s (4), (5), (6).

that a manipulator is, in essence, a system well adapted to acceleration transients but highly sensitive to steady-state-like high velocity requirements in the operational space.

Besides these conclusions we can make two important observations:

- While $g_{Q_1}(q_1)$ is a uniform p.d.f $g_{Q_2}(q_2)$ reveals maxima at $q_2 = \pm\pi/2$ and minima at $q_2 = \{0, \pm\pi\}$. This means that the kinematic structure 'prefers' the position configuration $q_2 = \pm\pi/2$ and 'avoids' $q_2 = \{0, \pm\pi\}$. As p.d.f. (4) is not responsible for this situation the result is an intrinsic property of the kinematic system.

- The $IP_{95}(\dot{q}_1)$ and $IP_{95}(\ddot{q}_1)$ have large amplitudes for $\mu < 1$ but stabilise for $\mu \geqslant 1$. On the other hand, the $IP_{95}(\dot{q}_2)$ and $IP_{95}(\ddot{q}_2)$ reveal minima at $\mu = 1$. Therefore, $\mu = 1$ (i.e. $l_1 = l_2$) is the kinematic structure of the 2R manipulator that minimises simultaneously the exigencies posed at both joints.

These experimental conclusions can be also inferred analytically. In fact, expressions (7) show that the larger the jacobian the smaller dispersion of o.v. In this case, the histogram tends to a collection of Dirac's and, if the histogram is centred on zero, this means average smaller amplitude requirements posed to that variable. Therefore, we have an optimisation criterion based on the statistical concepts that leads to an average reduction of the amplitude of the o.v.

The symbolic derivation of the jacobians requires the classical kinematic model. This indicates that the classical and the statistical models are *not exclusive* but are, in fact, *complementary*. Knowing that for the 2R manipulator the transformation $\mathbf{p} \rightarrow \mathbf{q}$ is given by the expression:

$$\begin{bmatrix} p_1 \\ p_2 \end{bmatrix} = \begin{bmatrix} l_1 C_1 + l_2 C_{12} \\ l_1 S_1 + l_2 S_{12} \end{bmatrix} \tag{9}$$

where $S_i = \sin(q_i)$ and $C_i = \cos(q_i)$, we get:

$$\mathfrak{J}_{P} = l_1 l_1 S_2 \tag{10a}$$

$$\mathfrak{J}_{P\dot{P}} = (l_1 l_1 S_2)^2 \tag{10b}$$

$$\mathfrak{J}_{P\dot{P}\ddot{P}} = (l_1 l_1 S_2)^3 \tag{10c}$$

The maximisation of $\mathfrak{J}_{P}$, $\mathfrak{J}_{P\dot{P}}$ and $\mathfrak{J}_{P\dot{P}\ddot{P}}$ requires the same steps. For:

$$L = l_1 + l_2 \tag{11a}$$

$$\mu = \frac{l_1}{l_2} \tag{11b}$$

a maximum occurs when

$$\mu = 1 \tag{12a}$$

$$q_2 = \pm\frac{\pi}{2} \tag{12b}$$

These expressions coincide with the numerical results and have distinct meanings:

- Condition (12a) defines the optimal kinematic structure of the 2R manipulator that must be optimised in a design stage
- Expression (12b) points out the best position configuration that must be satisfied through appropriate trajectory planning algorithms.

Such conclusions are similar to those obtained in previous studies [11–12] using the classical approach. Nevertheless, our method shows that if further optimisation is desired, then the next step will be the selection of optimal p.d.f.'s for the i.v.'s.

This second step of optimisation will define, in a statistical sense, an optimum kinematic class for the manipulator trajectories. Obviously, we can find a multitude of different p.d.f's obeying (12); nevertheless, for the subsequent study a particular choice is of minor importance. Consequently, to test numerically the statistical optimisation criterion, we adopted the following family of position p.d.f's in the operational space:

$$f_P(\mathbf{p}) = \frac{\chi}{\pi l_1 l_2}\left\{1 - \left[\frac{p_1^2 + p_2^2 - (l_1^2 + l_2^2)}{2l_1 l_2}\right]\right\}^{\frac{k-1}{2}} \tag{13a}$$

$$\chi = \begin{cases} \dfrac{1}{2\pi} & \text{if } k = 0 \\ \dfrac{1}{4} & \text{if } k = 1 \\ \dfrac{2\cdot 4\cdot 6\cdot \ldots \cdot k}{1\cdot 3\cdot 5\cdot \ldots \cdot k-1}\cdot\dfrac{1}{2\pi} & \text{if } k = 2, 4, 6, \cdots \\ \dfrac{1\cdot 3\cdot 5\ldots \cdot k}{2\cdot 4\cdot 6\cdot \ldots \cdot k-1}\cdot\dfrac{1}{4} & \text{if } k = 3, 5, 7, \cdots \end{cases} \tag{13b}$$

In the limit, for $k \to \infty$ we get:

$$f_P(\mathbf{p}) = \delta[p_1^2 + p_2^2 - (l_1^2 + l_2^2)] \tag{14}$$

where $\delta(\cdot)$ is the impulse of Dirac. In the joint space, the family of p.d.f.'s (13) and the limit case (14) correspond to:

$$g_Q(\mathbf{q}) = \chi |S_2|^k \tag{15}$$

$$g_Q(\mathbf{q}) = \frac{1}{2}\left[\delta\left(q_2 + \frac{\pi}{2}\right) + \delta\left(q_2 - \frac{\pi}{2}\right)\right] \tag{16}$$

The kinematic study does not point out any special class of p.d.f.'s for $\dot{\mathbf{p}}$ and $\ddot{\mathbf{p}}$. Nevertheless, these variables are affected negatively by the position deviation from the optimum configuration $q_2 = \pm\pi/2$. Therefore, in our experiments, we decided to compare the performances of an optimal $\mu = 1$ robot kinematic structure, for three different types of requirements in the operational space:

Case 1: The initial p.d.f.'s (4), (5) and (6);
Case 2: An 'enhanced' position p.d.f. (13) with $k = 3$ but maintaining the p.d.f.'s (5)–(6) for $\dot{\mathbf{p}}$ and $\ddot{\mathbf{p}}$;
Case 3: The 'enhanced' position p.d.f. (13) having $k = 3$ and 'enhanced' q_2-dependent velocity and acceleration p.d.f.'s:

$$f_{\dot{P}}(\dot{\mathbf{p}}, q_2) = \frac{1}{2\pi[\sigma_{\dot{P}}(q_2)]^2}\exp\left\{-\frac{\dot{p}_1^2 + \dot{p}_2^2}{2[\sigma_{\dot{P}}(q_2)]^2}\right\} \tag{17a}$$

$$\sigma_{\dot{P}}(q_2) = \begin{cases} \dfrac{2\sigma_{\dot{P}}|q_2|}{\pi} & \text{if } 0 \leqslant |q_2| \leqslant \dfrac{\pi}{2} \\ \dfrac{2\sigma_{\dot{P}}|q_2 - \pi|}{\pi} & \text{if } \dfrac{\pi}{2} < |q_2| \leqslant \pi \end{cases} \tag{17b}$$

$$f_{\ddot{\mathrm{p}}}(\ddot{\mathbf{p}}, q_2) = \frac{1}{2\pi[\sigma_{\ddot{\mathrm{p}}}(q_2)]^2} \exp\left\{-\frac{\ddot{p}_1^2 + \ddot{p}_2^2}{2[\sigma_{\ddot{\mathrm{p}}}(q_2)]^2}\right\} \tag{18a}$$

$$\sigma_{\ddot{\mathrm{p}}}(q_2) = \begin{cases} \dfrac{2\sigma_{\ddot{\mathrm{p}}}|q_2|}{\pi} & \text{if } 0 \leqslant |q_2| \leqslant \dfrac{\pi}{2} \\ \dfrac{2\sigma_{\ddot{\mathrm{p}}}|q_2 - \pi|}{\pi} & \text{if } \dfrac{\pi}{2} < |q_2| \leqslant \pi \end{cases} \tag{18b}$$

Figure 5 shows the IP_{95} index of the resulting histograms. The charts reveal a remarkable improvement of the kinematic performances particularly for velocity-dependent requirements. Therefore, beside demonstrating the validity of the optimisation criterion we have shown that the statistical modelling is not restricted to an analytic derivation but is also well suited to a numerical experimental-like study. This characteristic is of utmost importance because it allows not only the direct treatment of data from sensor measurements but also the alternative of symbolic *versus* numerical analysis.

3.2. The Dynamics

The dynamic phenomena correspond to the transformation $(\mathbf{q}, \dot{\mathbf{q}}, \ddot{\mathbf{q}}) \to \mathbf{T}$. The statistical description of this system requires steps similar to those adopted previously, namely characterisation of the i.v.'s $\mathbf{q}, \dot{\mathbf{q}}$ and $\ddot{\mathbf{q}}$ through appropriate p.d.f's and analysis of the o.v. $\mathbf{T}$. However, a preliminary observation shows that the dynamics is much more complex than the kinematics. Due to this reason, and in order to gain a deeper insight for the subsequent study we consider in a first stage, separately, the three sub-systems:

- $(\mathbf{q}, \dot{\mathbf{q}}, \ddot{\mathbf{q}}) \to \mathbf{T}$ with $g \neq 0$, $\dot{\mathbf{q}} = \mathbf{0}$ and $\ddot{\mathbf{q}} = \mathbf{0}$, that is the gravitational phenomena $\mathbf{q} \to \mathbf{T}_G$
- $(\mathbf{q}, \dot{\mathbf{q}}, \ddot{\mathbf{q}}) \to \mathbf{T}$ with $g = 0$, $\dot{\mathbf{q}} \neq \mathbf{0}$ and $\ddot{\mathbf{q}} = \mathbf{0}$, that is the Coriolis/centripetal phenomena $(\mathbf{q}, \dot{\mathbf{q}}) \to \mathbf{T}_C$
- $(\mathbf{q}, \dot{\mathbf{q}}, \ddot{\mathbf{q}}) \to \mathbf{T}$ with $g = 0$, $\dot{\mathbf{q}} = \mathbf{0}$ and $\ddot{\mathbf{q}} \neq \mathbf{0}$, that is the inertial phenomena $(\mathbf{q}, \ddot{\mathbf{q}}) \to \mathbf{T}_I$

Based on the insight given by this preliminary analysis then, in a second stage, we consider the total dynamic system $(\mathbf{q}, \dot{\mathbf{q}}, \ddot{\mathbf{q}}) \to \mathbf{T}$.

For the transformations $\mathbf{q} \to \mathbf{T}_G$, $(\mathbf{q}, \dot{\mathbf{q}}) \to (\mathbf{T}_G, \mathbf{T}_C)$ and $(\mathbf{q}, \dot{\mathbf{q}}, \ddot{\mathbf{q}}) \to (\mathbf{T}_G, \mathbf{T}_C, \mathbf{T}_I)$ we have:

$$h_{\mathrm{T_G}}(\mathbf{T}_G) = |\mathfrak{J}_Q| g_Q[\mathbf{q}(\mathbf{T}_G)] \tag{19a}$$

$$h_{\mathrm{T_G T_C}}(\mathbf{T}_G, \mathbf{T}_C) = |\mathfrak{J}_{Q\dot{Q}}| g_{Q\dot{Q}}[\mathbf{q}(\mathbf{T}_G, \mathbf{T}_C), \dot{\mathbf{q}}(\mathbf{T}_C)] \tag{19b}$$

$$h_{\mathrm{T_G T_C T_I}}(\mathbf{T}_G, \mathbf{T}_C, \mathbf{T}_I) = |\mathfrak{J}_{Q\dot{Q}\ddot{Q}}| g_{Q\dot{Q}\ddot{Q}}[\mathbf{q}(\mathbf{T}_G, \mathbf{T}_C, \mathbf{T}_I), \dot{\mathbf{q}}(\mathbf{T}_I)] \tag{19c}$$

where

$$\mathfrak{J}_Q = \frac{\partial(\mathbf{p})}{\partial(\mathbf{T}_G)} \tag{20a}$$

$$\mathfrak{J}_{Q\dot{Q}} = \frac{\partial(\mathbf{q}, \dot{\mathbf{q}})}{\partial(\mathbf{T}_G, \mathbf{T}_C)} \tag{20b}$$

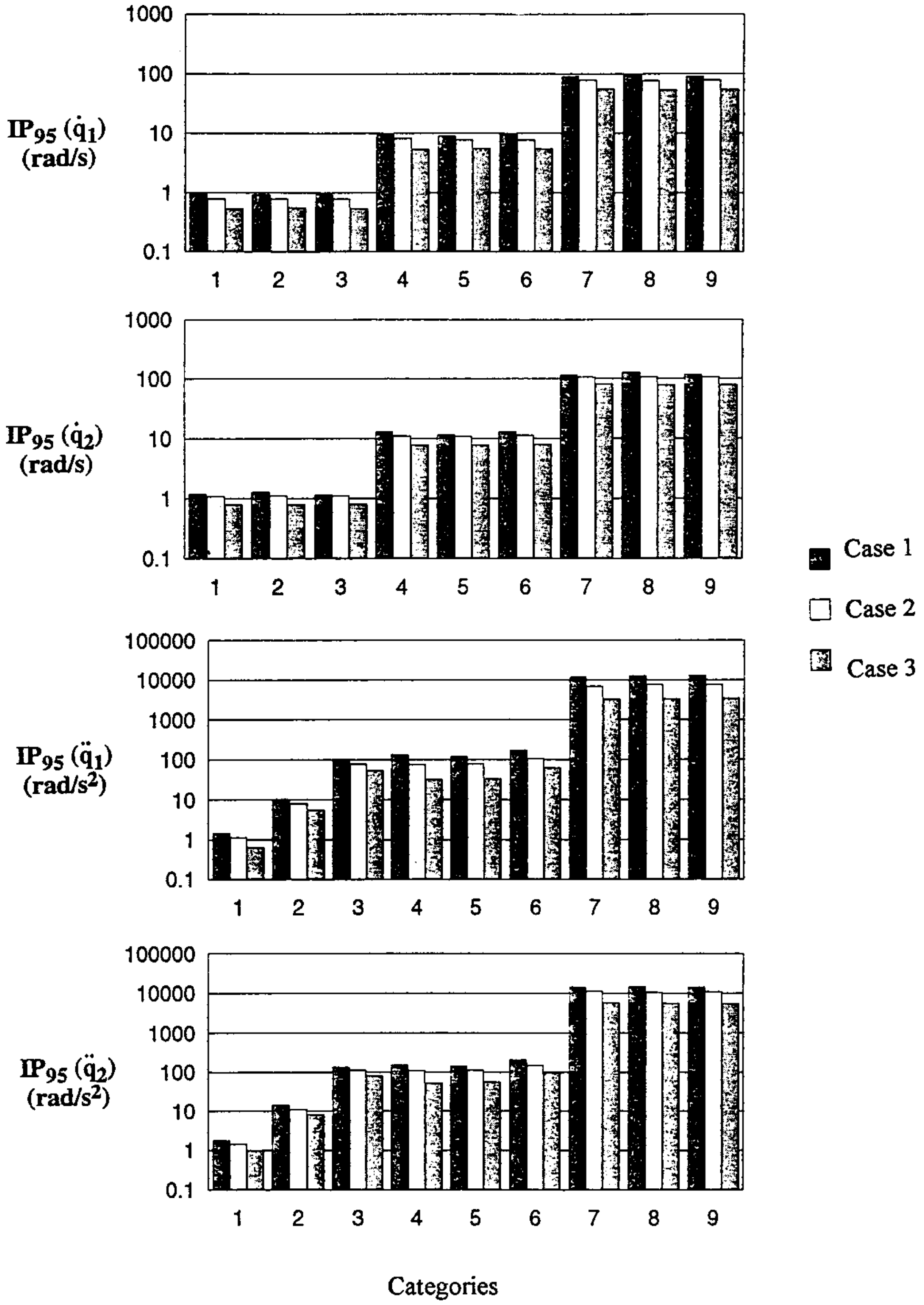

Figure 5 Comparison of the kinematic performances of the 2R manipulator with structure $\mu = 1$ for the p.d.f.'s:
Case 1–(4), (5), (6), Case 2–(13), (5), (6), Case 3–(13), (17), (18).

$$\mathfrak{J}_{Q\dot{Q}\ddot{Q}} = \frac{\partial(\mathbf{q}, \dot{\mathbf{q}}, \ddot{\mathbf{q}})}{\partial(\mathbf{T}_G, \mathbf{T}_C, \mathbf{T}_I)} \tag{20c}$$

Knowing that the classical dynamic model of the 2R manipulator gives:

$$\mathbf{I}(\mathbf{q}) = \begin{bmatrix} (m_1 + m_2)r_1^2 + m_2 r_2^2 + 2m_2 r_1 r_2 C_2 + J_1 & m_2 r_2^2 + m_2 r_1 r_2 C_2 \\ m_2 r_2^2 + m_2 r_1 r_2 C_2 & m_2 r_2{}^2 + J_2 \end{bmatrix} \tag{21a}$$

$$\mathbf{C}(\mathbf{q}, \dot{\mathbf{q}}) = \begin{bmatrix} -m_2 r_1 r_2 S_2 \dot{q}_2^2 - 2m_2 r_1 r_2 S_2 \dot{q}_1 \dot{q}_2 \\ m_2 r_1 r_2 S_2 \dot{q}_1^2 \end{bmatrix} \tag{21b}$$

$$\mathbf{G}(\mathbf{q}) = g \begin{bmatrix} m_1 r_1 C_1 + m_2 r_1 C_1 + m_2 r_2 C_{12} \\ m_2 r_2 C_{12} \end{bmatrix} \tag{21c}$$

then we can find that the analytical expressions of the jacobians:

$$\mathfrak{J}_Q = \{ [m_1 r_1 + (m_0 + m_2) l_1] (m_2 r_2 + m_0 l_2) g^2 S_1 S_{12} \}^{-1} \tag{22a}$$

$$\mathfrak{J}_{Q\dot{Q}} = \mathfrak{J}_Q \mathfrak{J}_{\dot{Q}} = \mathfrak{J}_Q \{ [2l_1(m_2 r_2 + m_0 l_2) S_2]^2 \dot{q}_1 \dot{q}_{12} \}^{-1} \tag{22b}$$

$$\mathfrak{J}_{Q\dot{Q}\ddot{Q}} = \mathfrak{J}_{Q\dot{Q}} \mathfrak{J}_{\ddot{Q}} = \mathfrak{J}_{Q\dot{Q}} \{ [J_1 + (m_2 + m_0) l_1^2] (J_2 + m_0 l_2^2) - [l_1^2 (m_2 r_2 + m_0 l_2) C_2]^2 \}^{-1} \tag{22c}$$

Unlike the kinematic situation, where the optimisation was similar for all the jacobians, now their effects differ according to each dynamic term. Analysing the jacobians (22) we conclude that:

- The maximising of $\mathfrak{J}_Q$ stipulates that $g_Q(\mathbf{q})$ should have maxima at $q_1 = \{0, \pm\pi\}$ or $q_{12} = \{0, \pm\pi\}$ and minima at $q_1 = \pm\pi/2$ or $q_{12} = \pm\pi/2$. The histograms $h_{T_{G_1}}(T_{G_1})$ and $h_{T_{G_2}}(T_{G_2})$ resulting from 'excitation' p.d.f.'s obeying these conditions resembled, as expected, Dirac impulses; however, those peaks were located at non-zero values. In fact, the plots showed sharp symmetrical peaks located at the maxima (positive and negative) amplitudes attained by the gravitational torques. Therefore, in this case, the optimisation procedure must minimise $\mathfrak{J}_Q$ which imposes that $g_Q(\mathbf{q})$ must have maxima at $q_1 = \pm\pi/2$ or $q_{12} = \pm\pi/2$ and minima at $q_1 = \{0, \pm\pi\}$ or $q_{12} = \{0, \pm\pi\}$.
- The maximising of $\mathfrak{J}_{\dot{Q}}$ implies that $g_Q(\mathbf{q})$ must have maxima at $q_2 = \{0, \pm\pi\}$. Numerical experiments showed that in this case the resulting histograms $h_{T_{C_1}}(T_{C_1})$ and $h_{T_{C_2}}(T_{C_2})$ tended, as desired, towards a Dirac on zero. In what concerns $\dot{\mathbf{q}}$ we observe that there is no optimising condition. Therefore, the smaller the requirements of $g_{\dot{Q}}(\dot{\mathbf{q}})$ the smaller the average amplitudes of T_{C_1} and T_{C_2}.
- The analytical expression of $\mathfrak{J}_{\ddot{Q}}$ reveals that $g_Q(\mathbf{q})$ must have maxima at $q_2 = \{0, \pm\pi\}$ and minima at $q_2 = \pm\pi/2$. In this case, experimentation demonstrated that a $g_Q(\mathbf{q})$ with maxima at $q_2 = \pm\pi$ and a minimum at $q_2 = 0$ leads to the best results on $h_{T_{I_1}}(T_{I_1})$ and $h_{T_{I_2}}(T_{I_2})$. On the other hand, there is no optimising condition on $\ddot{\mathbf{q}}$ which leads that the smaller the requirements of $g_{\ddot{Q}}(\ddot{\mathbf{q}})$ the smaller the average amplitudes of T_{I_1} and T_{I_2}.

In order to test these ideas we decided to 'excite' numerically the three subsystems, according with the synoptic diagram of Figure 6, with the position p.d.f.'s.

$$g_Q(\mathbf{q}) = (3/8)^2 |S_1 S_{12}|^3 \tag{23}$$

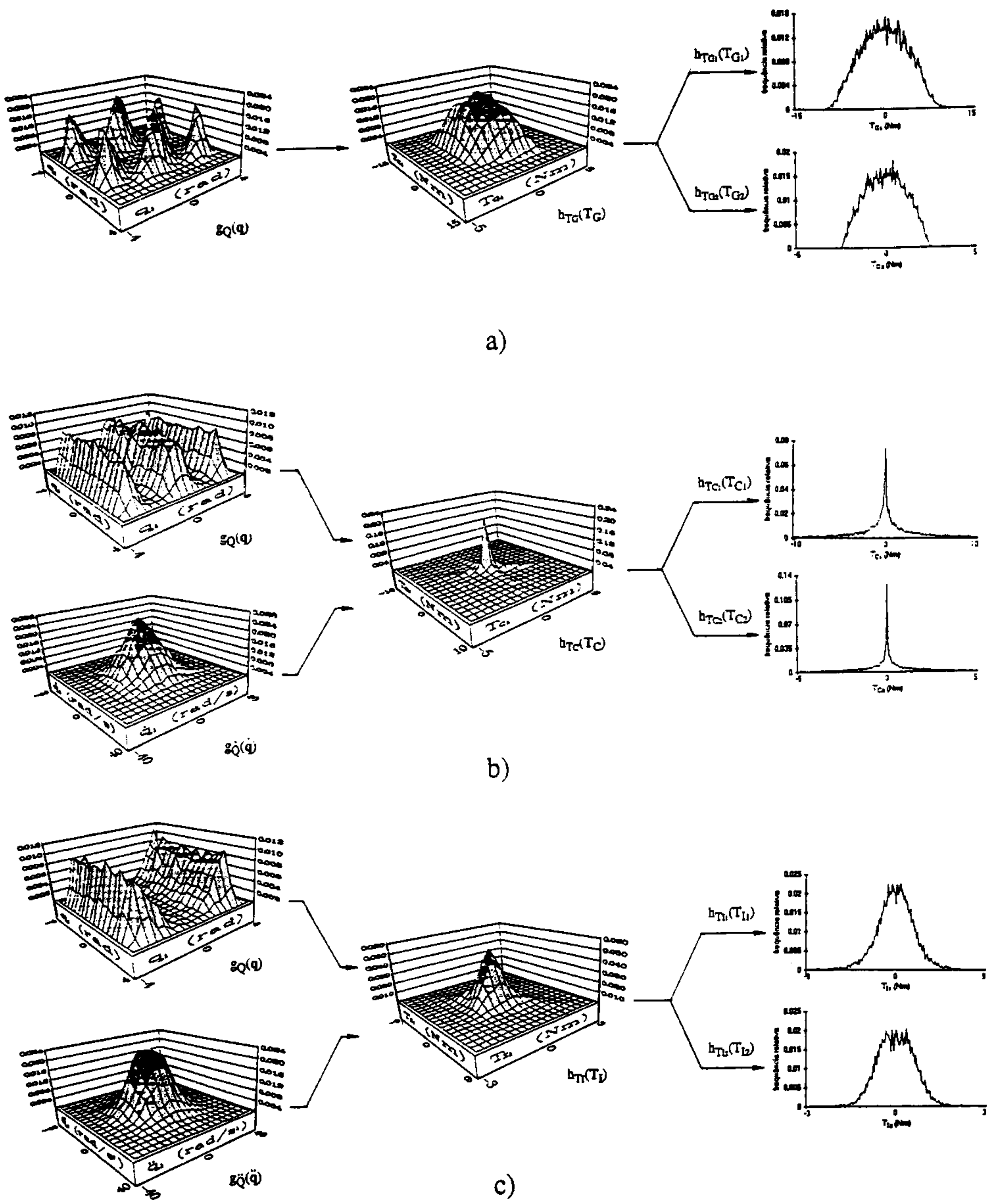

Figure 6 Synoptic diagram of the statistical modelling of the three dynamic sub-systems:
(a) The gravitational phenomena.
(b) The Coriolis/centripetal phenomena.
(c) The inertial phenomena.

$$g_Q(\mathbf{q}) = (3/8)\,|C_2|^3 \tag{24}$$

$$g_Q(\mathbf{q}) = (3/8)\,|S_{2/2}|^3 \tag{25}$$

$$g_Q(\mathbf{q}) = (3/8)\,|S_2|^3 \tag{26}$$

$$g_Q(\mathbf{q}) = (3/8)^2\,|S_1 S_2|^3 \tag{27}$$

where $S_{2/2} = \sin(q_2/2)$. The first three p.d.f.'s are suggested by the optimisation of the gravitational torques, the Coriolis/centripetal and inertial torques, respectively. The forth p.d.f. is already known and points to the optimisation of the kinematics. The fifth p.d.f. corresponds to a compromise between the optimisation of the kinematics and the gravitational torques. Due to the non-existence of optimisation guidelines on $\dot{\mathbf{q}} = [\dot{q}_1, \dot{q}_2]^T$ and $\ddot{\mathbf{q}} = [\ddot{q}_1, \ddot{q}_2]^T$, we decided to consider two Gaussian 'excitation' p.d.f.'s:

$$g_{\dot{Q}}(\dot{\mathbf{q}}) = \frac{1}{2\pi\sigma_{\dot{Q}}^2} \exp\left(-\frac{\dot{q}_1^2 + \dot{q}_2^2}{2\sigma_{\dot{Q}}^2}\right) \tag{28}$$

$$g_{\ddot{Q}}(\ddot{\mathbf{q}}) = \frac{1}{2\pi\sigma_{\ddot{Q}}^2} \exp\left(-\frac{\ddot{q}_1^2 + \ddot{q}_2^2}{2\sigma_{\ddot{Q}}^2}\right) \tag{29}$$

and the sixteen different categories of requirements represented in Table III:

Table III Requirements of $\dot{\mathbf{q}}$ and $\ddot{\mathbf{q}}$.

Category	*1*	*2*	*3*	*4*	*5*	*6*	*7*	*8*	*9*	*10*	*11*	*12*	*13*	*14*	*15*	*16*
$\sigma_{\dot{Q}_1}$	0.1	0.1	0.1	0.1	0.1	0.1	0.1	0.1	10	10	10	10	10	10	10	10
$\sigma_{\dot{Q}_2}$	0.1	0.1	0.1	0.1	10	10	10	10	0.1	0.1	0.1	0.1	10	10	10	10
$\sigma_{\ddot{Q}_1}$	0.1	0.1	10	10	0.1	0.1	10	10	0.1	0.1	10	10	0.1	0.1	10	10
$\sigma_{\ddot{Q}_2}$	0.1	10	0.1	10	0.1	10	0.1	10	0.1	10	0.1	10	0.1	10	0.1	10

Figures 7 to 9 show the results of the experiments condensed through the IP_{95} index. Due to the symmetry of the histograms only the positive half is presented. As expected, p.d.f.'s (23), (24) and (25) reveal superior performances for the corresponding phenomena.

Based on the analysis of the partial phenomena, now we can proceed to the second

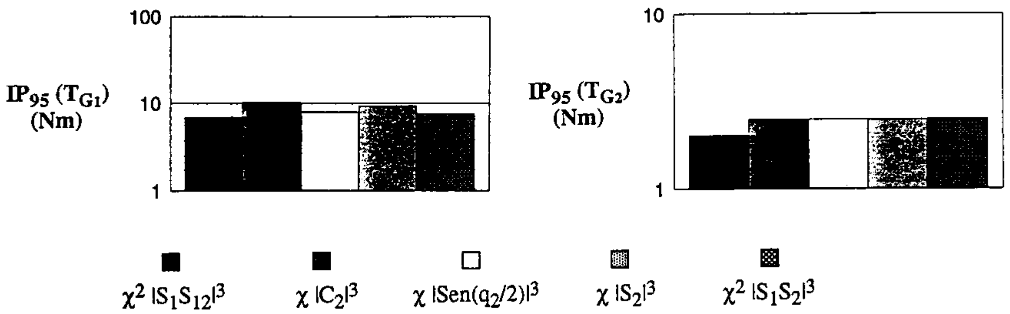

Figure 7 Comparison of the gravitational performances of the 2R manipulator with structure $\mu = 1$ for the p.d.f.'s (23)–(27).

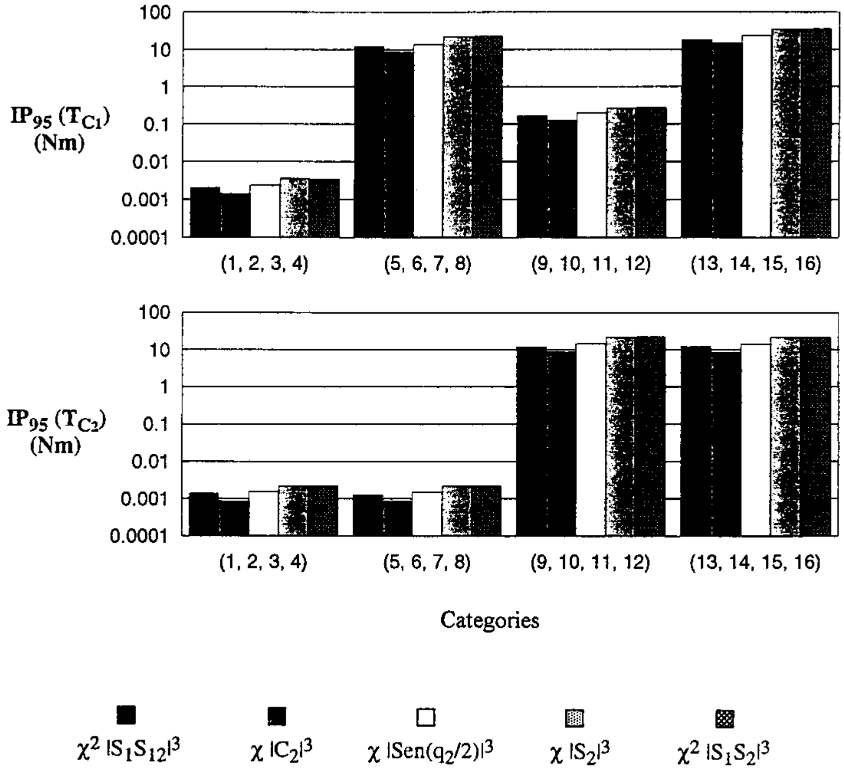

Figure 8 Comparison of the Coriolis/centripetal performances of the 2R manipulator with structure $\mu = 1$ for the p.d.f.'s (23)-(27) and (28).

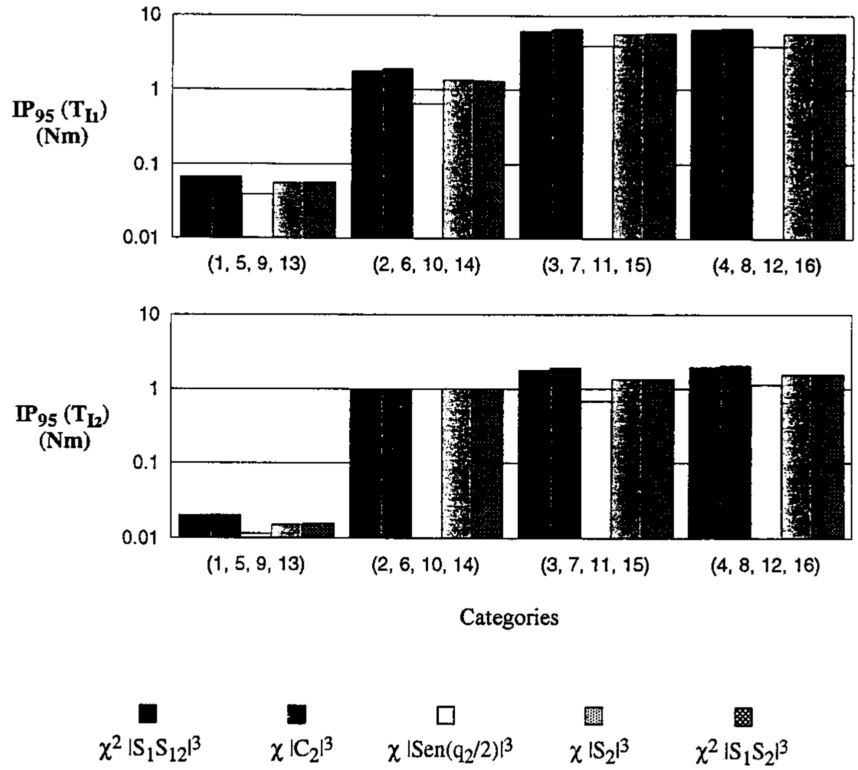

Figure 9 Comparison of the inertial performances of the 2R manipulator with structure $\mu = 1$ for the p.d.f.'s (23)-(27) and (29).

stage, that is, the study of (total) dynamics. The direct application of our method to the relation $(\mathbf{q}, \dot{\mathbf{q}}, \ddot{\mathbf{q}}) \rightarrow \mathbf{T}$ would require the treatment of $3n$-dimensional p.d.f.'s. To avoid this intricate analysis, we decided to integrate heuristically the conclusions pointed out in the first stage of the present investigation. This approximate scheme allows the numerical evaluation of the relative weight of the partial dynamic phenomena and shows that, with the statistical model, we can go round laborious analytical exercises. In this sense, we 'excited' the dynamics with random samples of points obeying the p.d.f.'s (23)-(29) considered in the first phase. Figure 10 depicts the positive half of $IP_{95}(T_1)$ and $IP_{95}(T_2)$ of the resulting histograms. These charts reveal that:

- T_1 depends strongly on $\dot{q}_2$
- T_2 depends strongly on $\dot{q}_1$

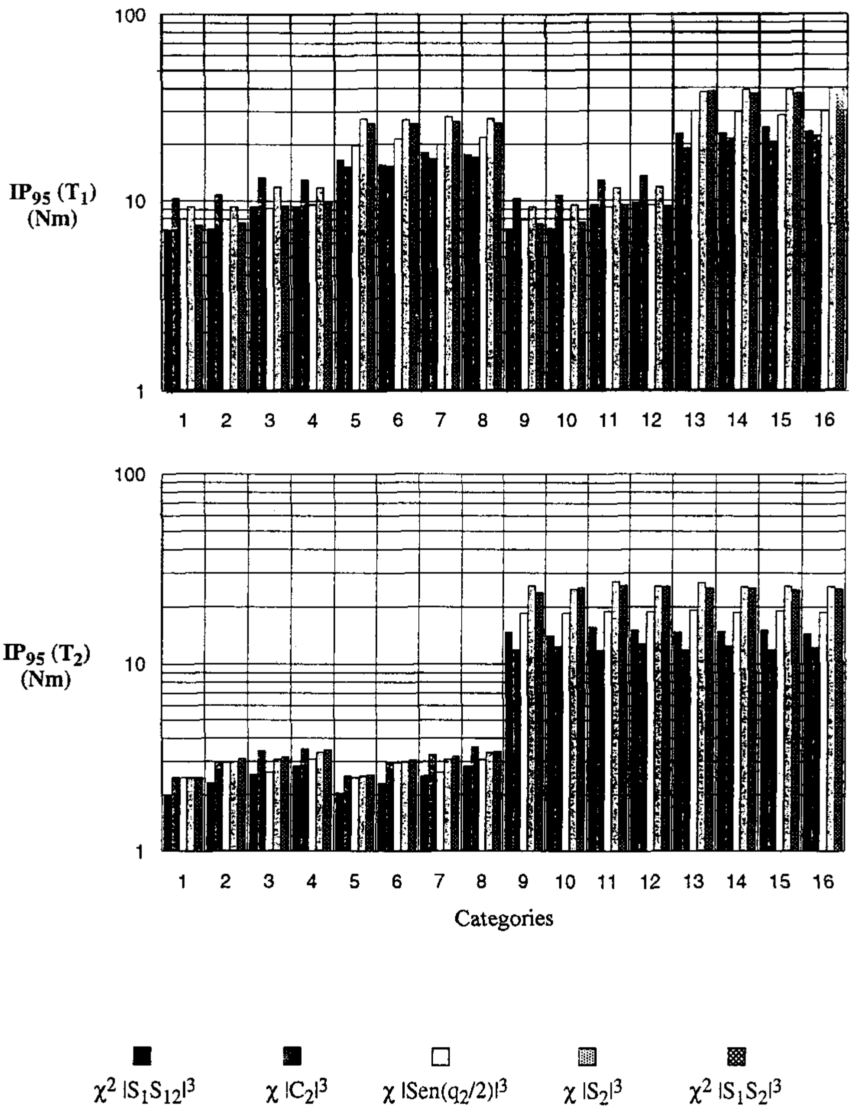

Figure 10 Comparison of the total dynamic performances of the 2R manipulator with structure $\mu = 1$ for the p.d.f.'s (23)-(27), (28) and (29).

- The joint torques $\mathbf{T}$ have low sensitivity to requirements on $\ddot{\mathbf{q}}$
- In average, the gravitational torques are a significant component of the total torques

In conclusion, the multidimensional properties of the dynamics, where co-exist phenomena of different nature, makes difficult the appearance of a common optimising pattern.

The final step of our study will be the evaluation of the accumulated effects of the kinematics and dynamics and to what extend we can make compatible the contradictory optimising rules.

3.3. *The Global System*

The description of the global system will have cross-coupling effects between the kinematics and the dynamics. This case corresponds to the study of the transformation $(\mathbf{p}, \dot{\mathbf{p}}, \ddot{\mathbf{p}}) \rightarrow \mathbf{T}$ and its statistical treatment requires the definition of appropriate p.d.f.'s for the i.v.'s. From the results of the previous sub-sections, we decided to test the system for five $f_P(\mathbf{p})$ corresponding to p.d.f.'s (23)–(27) in the joint space. By other words, knowing that:

$$f_P(\mathbf{p}) = \left| \frac{\partial(\mathbf{q})}{\partial(\mathbf{p})} \right| g_Q[\mathbf{p}(\mathbf{q})] \tag{30}$$

we are adopting p.d.f.'s for $\mathbf{p}$ such that (Figure 11):

$$f_P(\mathbf{p})^A \leftrightarrow g_Q(\mathbf{q})^A = (3/8)^2 |S_1 S_{12}|^3 \tag{31}$$

$$f_P(\mathbf{p})^B \leftrightarrow g_Q(\mathbf{q})^B = (3/8)\, |C_2|^3 \tag{32}$$

$$f_P(\mathbf{p})^C \leftrightarrow g_Q(\mathbf{q})^C = (3/8)\, |S_{2/2}|^3 \tag{33}$$

$$f_P(\mathbf{p})^D \leftrightarrow g_Q(\mathbf{q})^D = (3/8)\, |S_2|^3 \tag{34}$$

$$f_P(\mathbf{p})^E \leftrightarrow g_Q(\mathbf{q})^E = (3/8)^2 |S_1 S_2|^3 \tag{35}$$

On the other hand, for $f_{\dot{P}}(\dot{\mathbf{p}})$ and $f_{\ddot{P}}(\ddot{\mathbf{p}})$ we considered the Gaussian p.d.f.'s (5) and (6), respectively, and the nine categories of requirements presented in Table II. The synoptic diagram of Figure 12 illustrate the corresponding numerical experiments. The results (Figure 13) reveal that:

- For low requirements of $\dot{\mathbf{p}}$ and $\ddot{\mathbf{p}}$ (category 1), the IP_{95} index gives almost similar results for all p.d.f.'s, because the gravitational torques predominate.
- Requirements on $\dot{\mathbf{p}}$ have a much stronger influence than requirements on $\ddot{\mathbf{p}}$.
- Kinematic effects prevail over the Coriolis/centripetal and inertial phenomena. Therefore, the best results come from $f_P(\mathbf{p})^E$ that is from the compromise between kinematic and gravitational phenomena.

In conclusion, the statistical analysis reveals that the kinematics and dynamics have different effects upon the robot system. As shown, mechanical manipulators are much more sensitive to velocity requirements than to acceleration requirements and, for fast movements, kinematics is far more significant than dynamics. These facts indicate that we are dealing with acceleration/deceleration transient-like systems rather than steady-state velocity devices. Although obvious, this aspect has been somewhat overlooked. Moreover, it points out that the usual robot actuators,

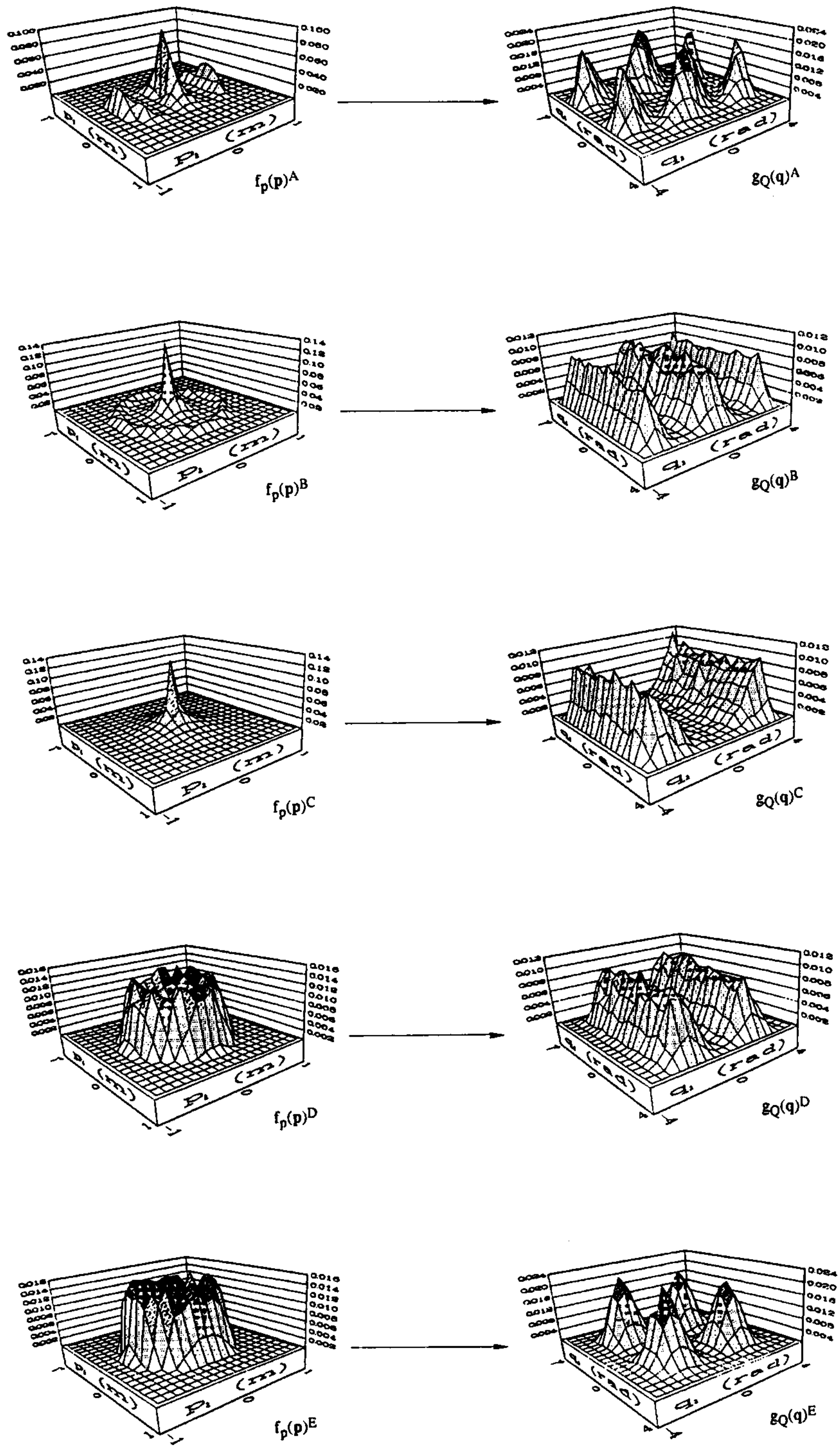

Figure 11 Representation in the operational and joint spaces of the five position p.d.f.'s under evaluation.

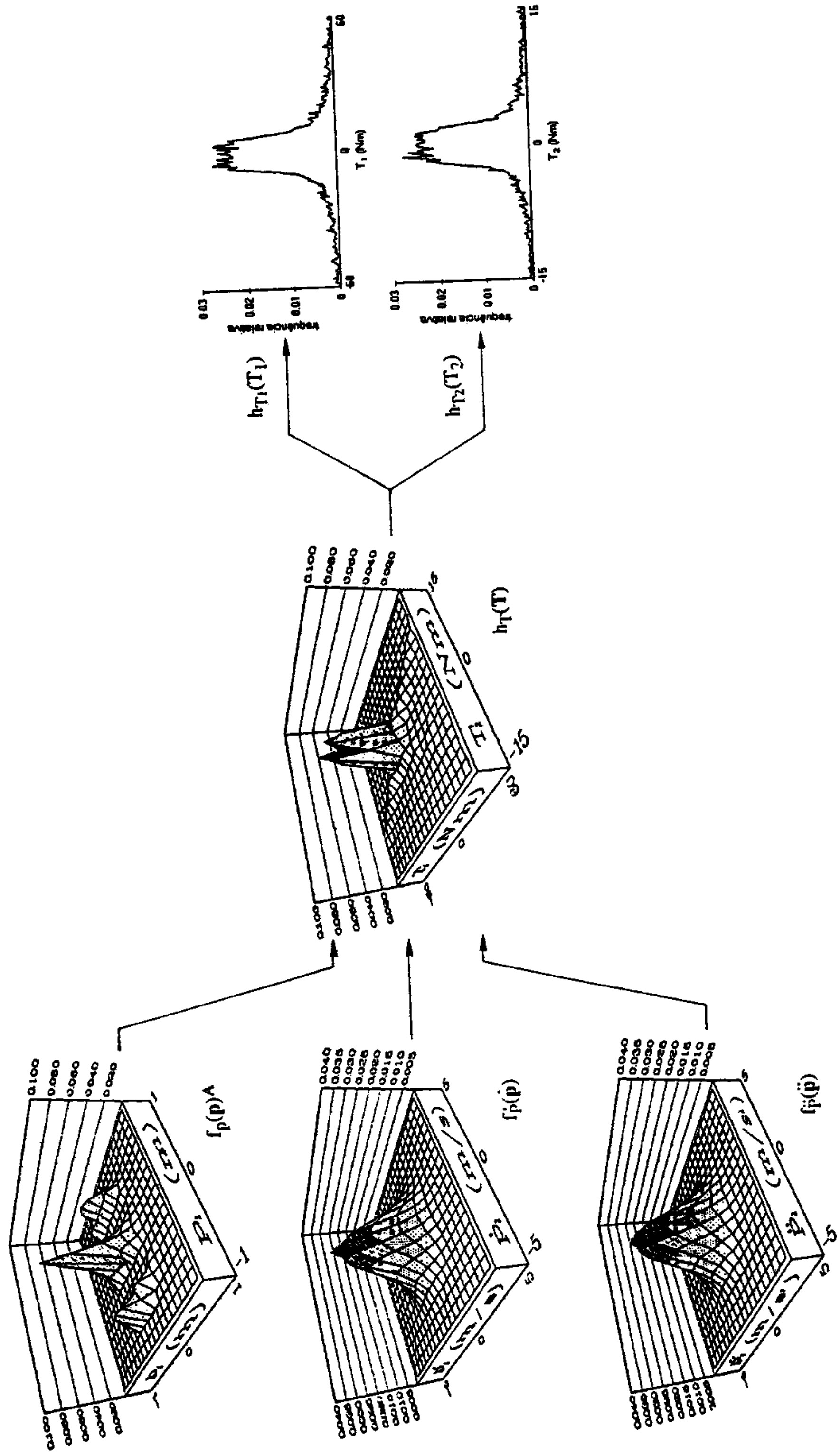

Figure 12 Synoptic diagram of the statistical modelling of the global system.

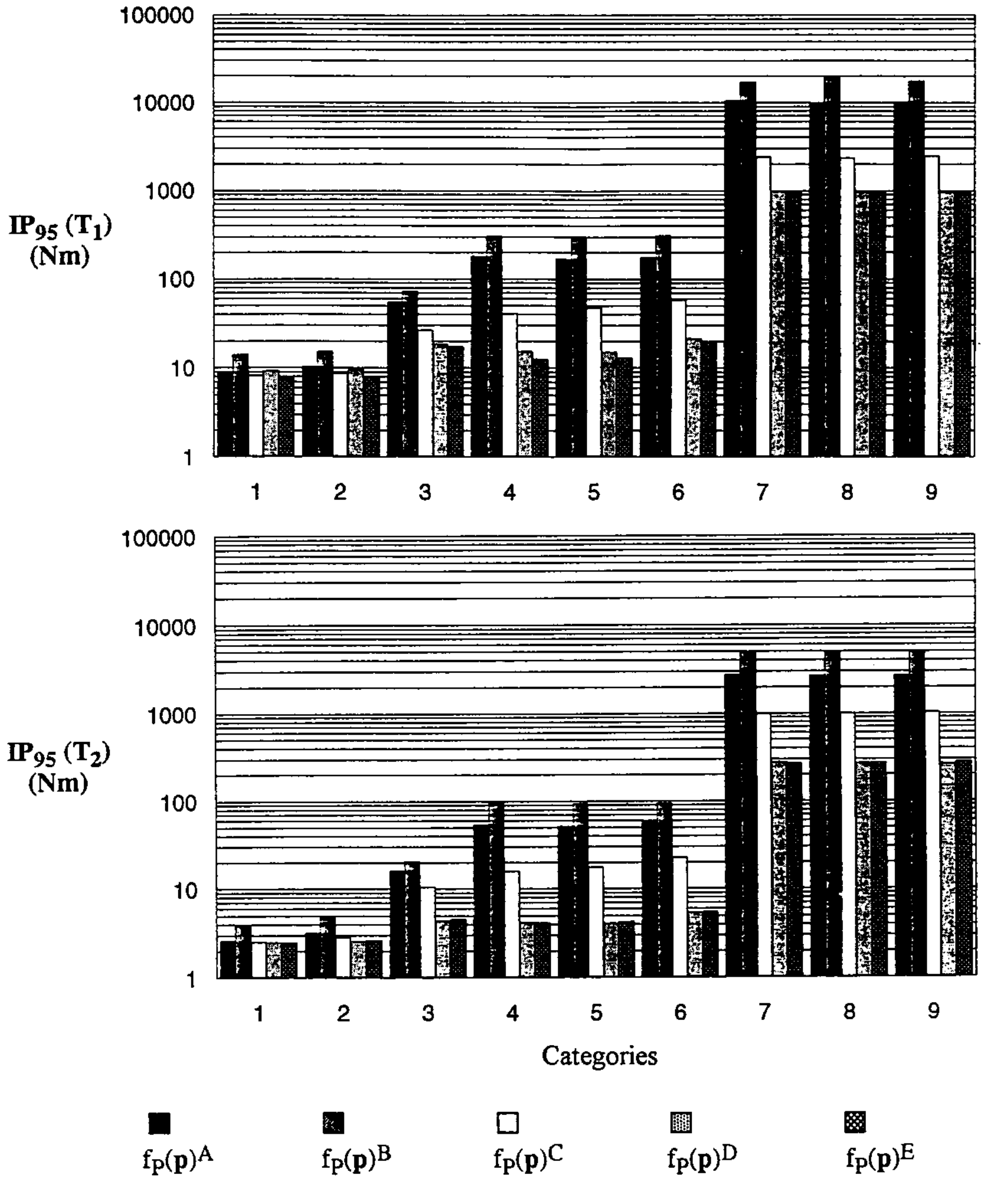

Figure 13 Comparison of the global performances of the 2R manipulator with structure $\mu = 1$ for the p.d.f.'s (31)-(35), (5) and (6).

which are developments of standard steady-state electrical machines are not well adapted to robotic applications. Alternative solutions, such as muscle like actuators will allow more efficient robot structures [24-25].

4. CONCLUSIONS

A new method to the analysis and design of robot manipulators was announced. The novel feature resides on a non standard approach to the modelling problem. Usually, system descriptions are based on a set of differential equations which, due to their nature lead to very precise results but can be very complex and hard to tackle. These difficulties motivate the development of models having distinct characteristics. The statistical formalism is a step in that direction which has been shown to give clear guidelines towards the optimisation both of the path planning algorithm and the robot structure. Furthermore, the results point out structural characteristics that define robotic manipulators as acceleration-based systems. Therefore, joint-actuated arms are non-optimal systems and alternative structures with linear muscle-like actuators and appropriate mechanical levers are the key reference for the development of more efficient manipulating systems.

References

[1] Luh, J. Y. S.; Walker, M. W.; Paul, R. P. C.: *On-Line Computational Scheme for Mechanical Manipulators*, ASME J. Dynamic Syst., Meas., Contr., vol. 102, pp. 69–76, June 1980.
[2] John M. Hollerbach: *A Recursive Lagrangian Formulation of Manipulator Dynamics and a Comparative Study of Dynamics Formulation Complexity*, IEEE Trans. Syst., Man, Cybern., vol. SMC-10, pp. 730–736, Nov. 1980.
[3] Charles P. Neuman; John J. Murray: *The Complete Model and Customized Algorithms of the Puma Robot*, IEEE Trans. Syst., Man, Cybern., vol. SMC-17, pp. 635–644, July/Aug. 1987.
[4] Leu, M. C.; Hemati, N.: *Automated Symbolic Derivation of Dynamic Equations of Motion for Robotic Manipulators*, ASME J. Dynamic Syst. Meas. Contr., vol. 108, pp. 172–179, Sept. 1986.
[5] Koplic, J.; Leu, M. C.: *Computer Generation of Robot Dynamic Equations and the Related Issues*, J. of Robotic Systems, vol. 3, n. 3, pp. 301–319, Fall 1986.
[6] Charles P. Neuman; John J. Murray: *Customized Computational Robot Dynamics*, J. of Robotic Systems, vol. 4, n. 4, pp. 503–526, Aug. 1987.
[7] Charles P. Neuman; John J. Murray: *Symbolically Efficient Formulations for Computational Robol Dynamics*, J. of Robotic Systems, vol. 4, n. 6, pp. 743–769, Dec. 1987.
[8] Pi-Ying Cheng; Cheng-I Weng; Chao-Kuang Chen: *Symbolic Derivation of Dynamic Equations of Motion for Robot Manipulators Using Program Symbolic Method*, IEEE J. of Robotics and Automation, vol. 4, no. 6, pp. 599–609, Dec. 1988.
[9] Armstrong, B.; Khatib, O.; Burdick, J.: *The Explicit Dynamic Model and Inertial Parameters of the PUMA 560 Arm*, Proc. 1986 IEEE Int. Conf. on Robotics and Automation, San Francisco, CA, 1986.
[10] Tenreiro Machado, J. A.; Martins de Carvalho, J. L.: *Microprocessor-Based Controllers for Robotic Manipulators*, in *Microprocessors in Robotic and Manufacturing Systems*, Kluwer Academic Publishers (editor: Spyros G. Tzafestas), 1991.
[11] Tsai, Y. C.; Soni, A. H.: *Accessible Region and Synthesis of Robot Arms*, ASME J. Mech. Design, vol. 103, pp. 803–811, October 1981.
[12] Tsuneo Yoshikawa: *Manipulability of Robotic Mechanisms*, The Int. J. Robotics Research, vol. 4, n. 2, pp. 3–9, Summer 1985.
[13] Haruhiko Asada: *A Geometrical Representation of Manipulator Dynamics and its Application to Arm Design*, ASME J. Dynamic Syst., Meas., Contr., vol. 105, pp. 131–142, September 1983.
[14] Tsuneo Yoshikawa: *Analysis and Design of Articulated Robot Arms from the Viewpoint of Dynamic Manipulability*, Robotics Research, The Third Int. Symp., pp. 273–279, 1986.
[15] Yang, D. C. H.; Tzeng, S. W.: *Simplification and Linearization of Manipulator Dynamics by the Design of Inertia Distribution*, The Int. Robotics Research, vol. 5, n. 3, pp. 120–128, Fall 1986.
[16] Kamal Youcef-Toumi; Haruhiko Asada: *The Design of Open-Loop Manipulator Arms With Decoupled and Configuration-Invariant Inertia Tensors*, ASME J. Dynamic Syst. Meas., Contr., vol. 109, n. 3, pp. 268–275, September 1987.
[17] Hollerbach, J. M.: *Dynamic Scaling of Manipulator Trajectories*, ASME J. Dyn. Syst. Meas., Contr., vol. 106, pp. 102–106, March 1984.
[18] Gideon Sahar; John M. Hollerbach: *Planning of Minimum-Time Trajectories for Robot Arms*, The Int. J. R. Research, vol. 5, n. 3, pp. 90–100, Fall 1986.
[19] Scheinman, V.; Roth, B.: *On the Optimal Selection and Placement of Manipulators*, Proc. RoManSy, Udine, Italy, 1984.
[20] Mooring, B. W.; Pack, T. J.: *Aspects of Robot Repeatability*, Robotica, vol. 5, Part 3, pp. 223–230, July–September 1987.

[21] Alexandra M. S. F. Galhano; Tenreiro Machado, J. A.; Martins de Carvalho, J. L.: *On the Analysis and Design of Robot Manipulators: A Statistical Approach*, 11th IFAC World Congress, Tallinn, USSR, 1990.

[22] Alexandra, M. S. F. Galhano; Martins de Carvalho, J. L.; Tenreiro Machado, J. A.: *On the Statistical Analysis of Mechanical Manipulators*, 13th IMACS World Congress on Computation and Applied Mathematics, Dublin, Ireland, 1991.

[23] Alexandra M. S. F. Galhano; Tenreiro Machado, J. A.; Martins de Carvalho, J. L: *On the Statistical Modelling of Mechanical Manipulators*, IFAC/IFIP/IMACS. Symposium on Robot Control SYROCO'91, Vienna, Austria, 1991.

[24] Alexandra M. S. F. Galhano; Tenreiro Machado, J. A.; Martins de Carvalho, J. L.: *On the Statistical Analysis and Design of Robot Manipulators: A Statistical Perspective*, IEEE Int. Symp. on Advanced Motion Control, Yokohama, Japan, 1990.

[25] Alexandra M. S. F. Galhano; Tenreiro Machado, J. A.; Martins de Carvalho, J. L.: *Statistical Analysis of Muscle-Actuated Manipulators*, IEEE Int. Conf. on Robotics and Automation, Nice, France, 1992.